

Supporting Information

From aggregation-induced to solution emission: A new strategy for designing ratiometric fluorescent probes and its application for *in vivo* HClO detection

Rongguang shi, ^a Hua Chen, ^b Yunpeng Qi, ^b Wei Huang, ^{*a} Gui Yin^{*a} and Ruiyong Wang^{*b}

- a. *State Key Laboratory of Coordination Chemistry, State Key Laboratory of Analytical Chemistry for Life Science, School of Chemistry and Chemical Engineering, Nanjing University, Nanjing, 210093, People's Republic of China. E-mail: whuang@nju.edu.cn, yingui@nju.edu.cn.*
- b. *State Key Laboratory of Pharmaceutical Biotechnology, School of Life Science, Nanjing University, Nanjing, 210093, People's Republic of China. E-mail: wangry@nju.edu.cn.*

Contents

1. Fluorescence and UV-vis spectra affected by AIE
2. Mechanism research
3. Detection limit calculation
4. Determination of reaction time
5. pH-dependent research
6. Cytotoxicity study
7. Cell imaging
8. Crystal data of PDAM-Me
9. Supplemental spectra

1. Fluorescence and UV-vis spectra affected by AIE

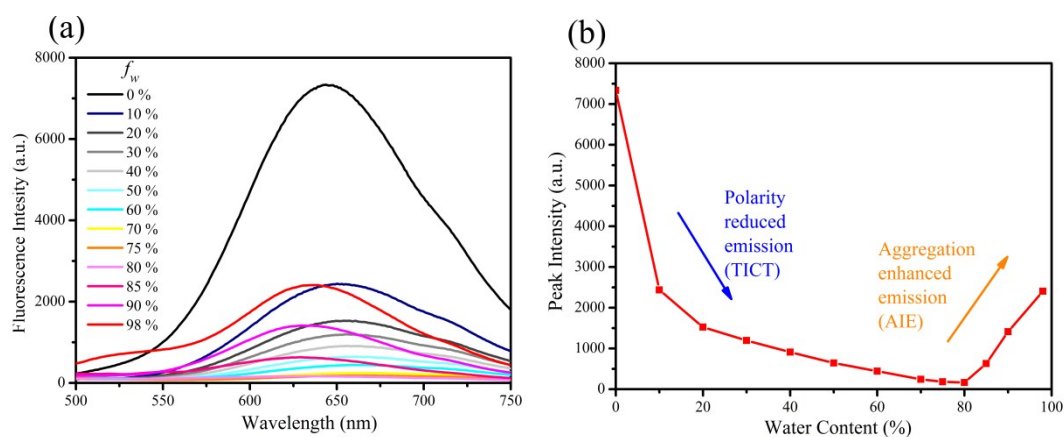


Fig. S1 (a) Fluorescence spectra of PDAM-Me in the MeCN-water mixtures with different water contents ($\lambda_{\text{ex}} = 410$ nm). (b) Fluorescence peak intensity of PDAM-Me *versus* water content of the solvent mixture.

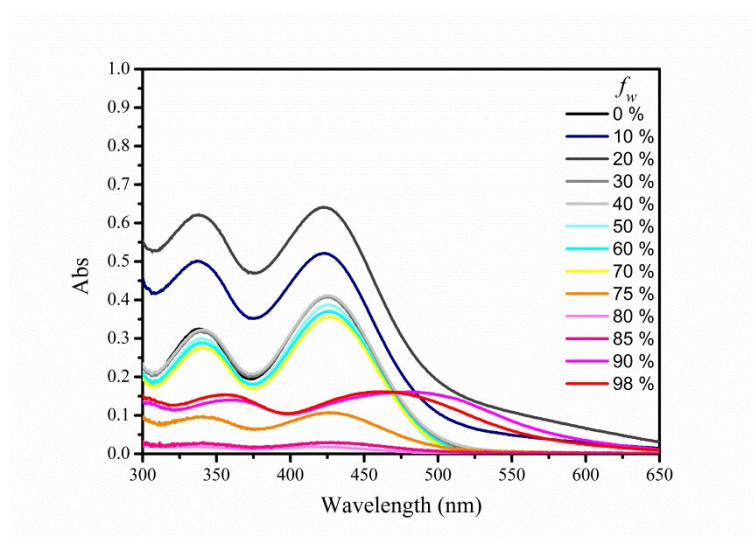


Fig. S2 UV-vis spectra of PDAM-Lyso (20 μM) in CH_3CN , upon increasing volume percentages of water from 0% to 98%.

2. Mechanism research

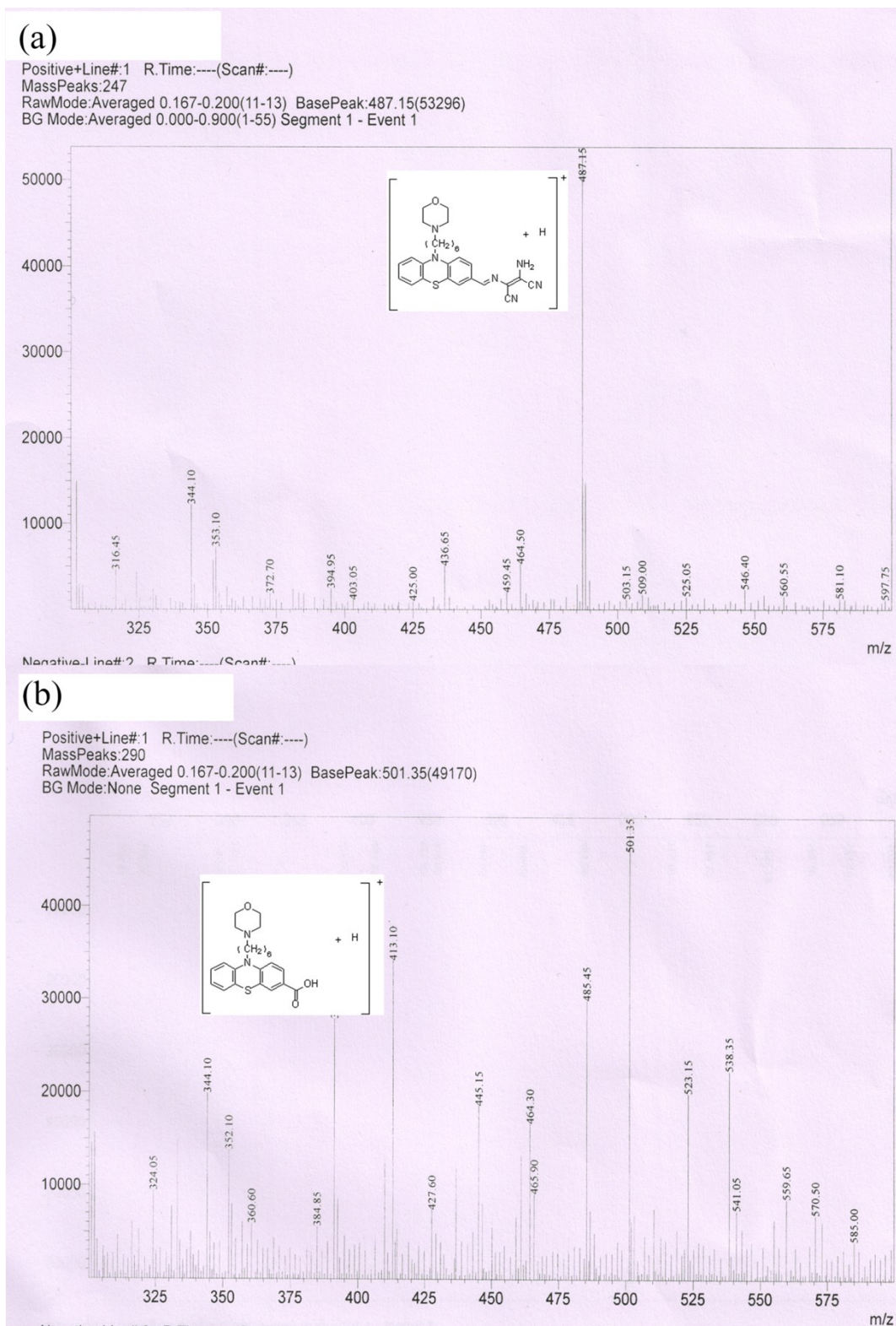


Fig.S3 (a) LCMS spectra of PDAM-Lyso. (b) LCMS spectra of PDAM-Lyso + NaClO.

3. Detection limit calculation

Fluorescence titration was carried out in CH₃CN/PBS buffer (1/9, v/v, 10 mM, pH = 7.4) to determine the detection limit, which was then calculated with the equation:

$$\text{Detection of limit} = 3b_i/m$$

where b_i is the standard deviation of blank measurements and is calculated with twenty ($n = 20$) experiments, and m is the slope between intensity ration (I_{470}/I_{620}) and sample concentration. It was calculated that the detection limit was 440 nm.

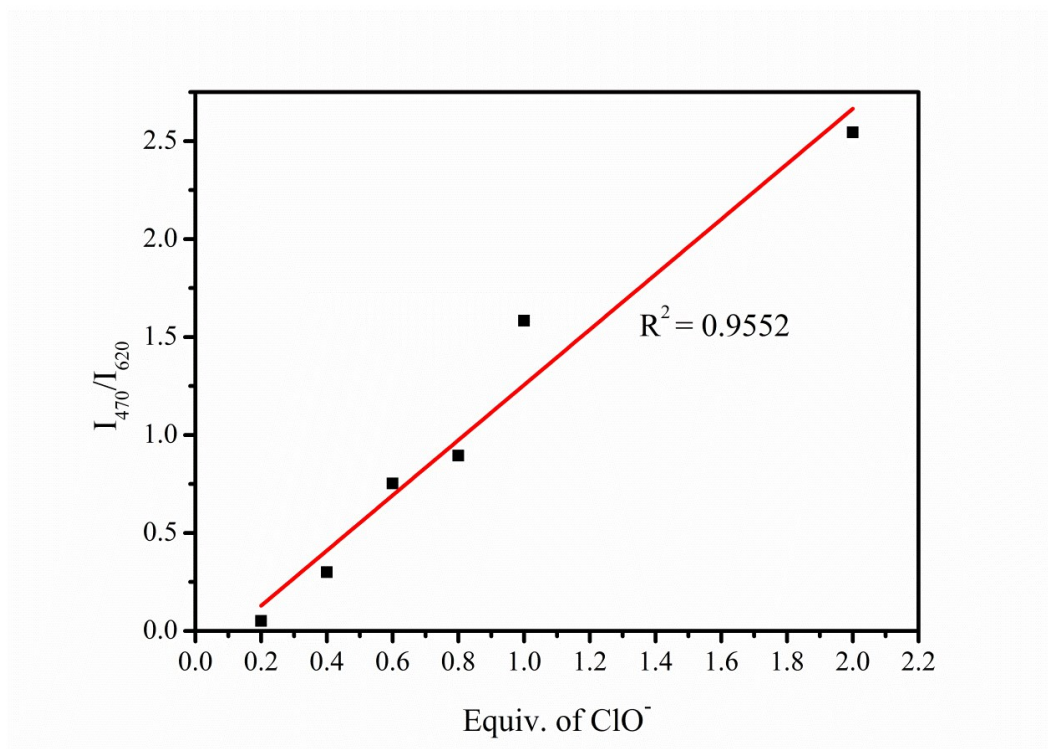


Fig. S4 The dependence curve of fluorescence intensity ratios (I_{470}/I_{620}) in the presence of ClO⁻ in CH₃CN/PBS buffer (1/9, v/v, 10 mM, pH = 7.4), ($\lambda_{\text{ex}} = 410$ nm).

4. Determination of reaction time

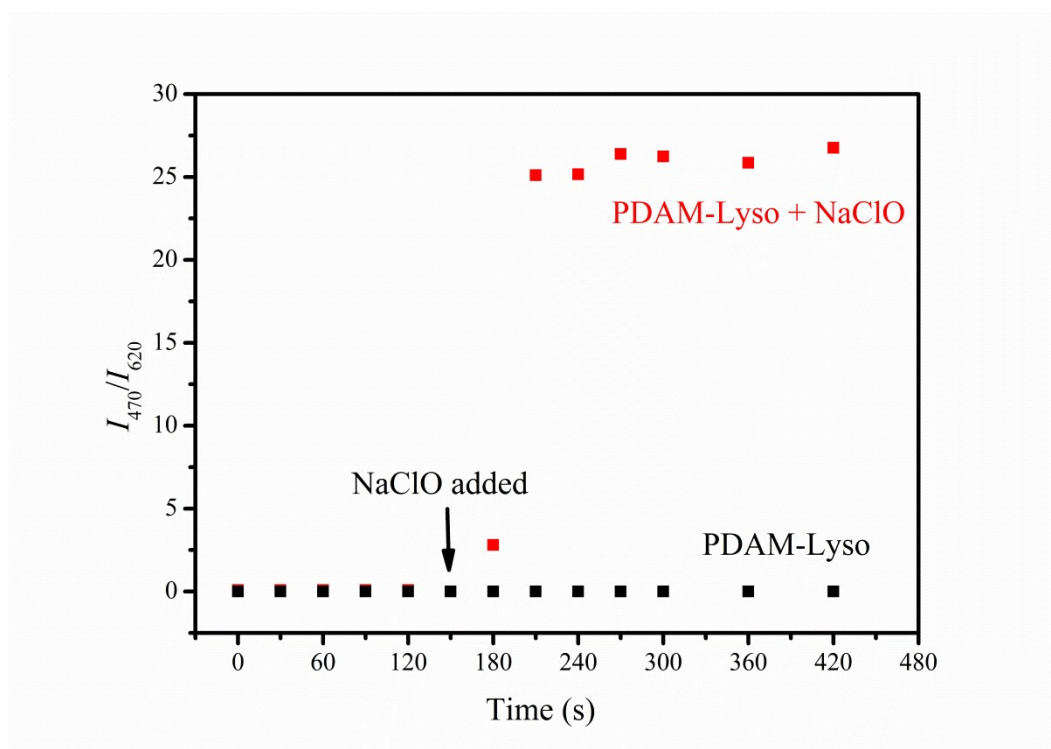


Fig. S5 Reaction-time profiles of PDAM-Lyso (20 μ M) in the absence and presence of NaClO in $\text{CH}_3\text{CN}/\text{PBS}$ buffer (1/9, v/v, 10 mM, pH = 7.4) (λ_{ex} =410 nm).

5. pH-dependent research

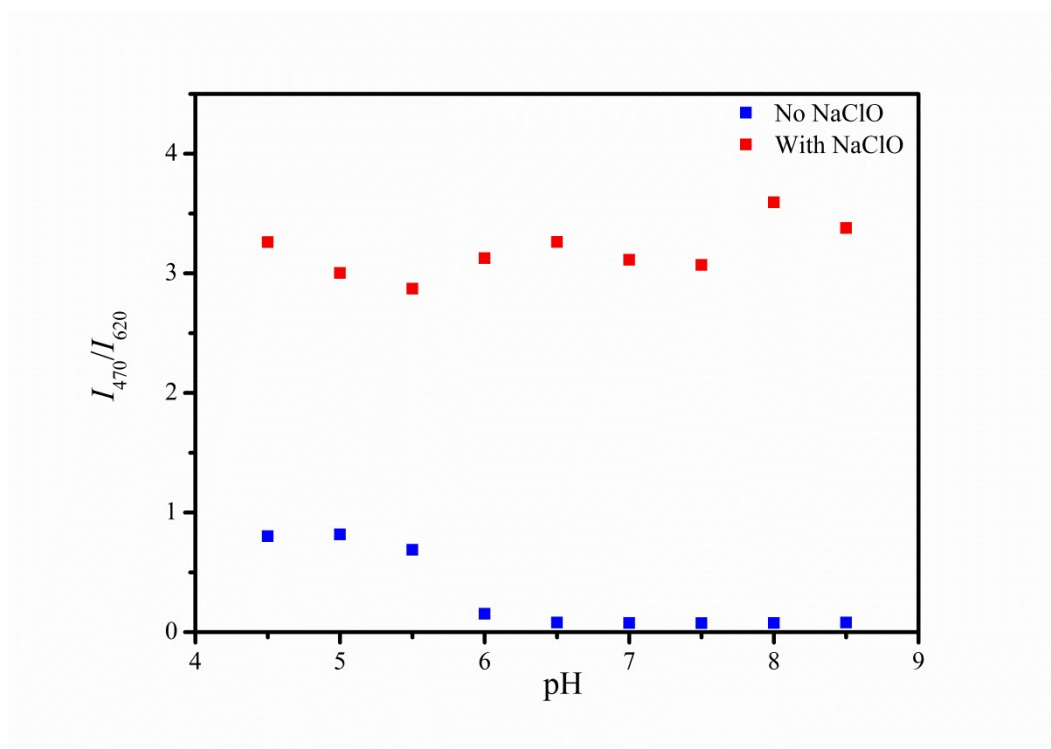


Fig. S6 pH-dependent profiles of PDAM-Lyso (20 μ M) in the absence and presence of NaClO (2.5 eq.) with pH range of 4.5 – 8.5 in $\text{CH}_3\text{CN}/\text{PBS}$ buffer (1/9, v/v, 10 mM) (λ_{ex} =410 nm).

6. Cytotoxicity study

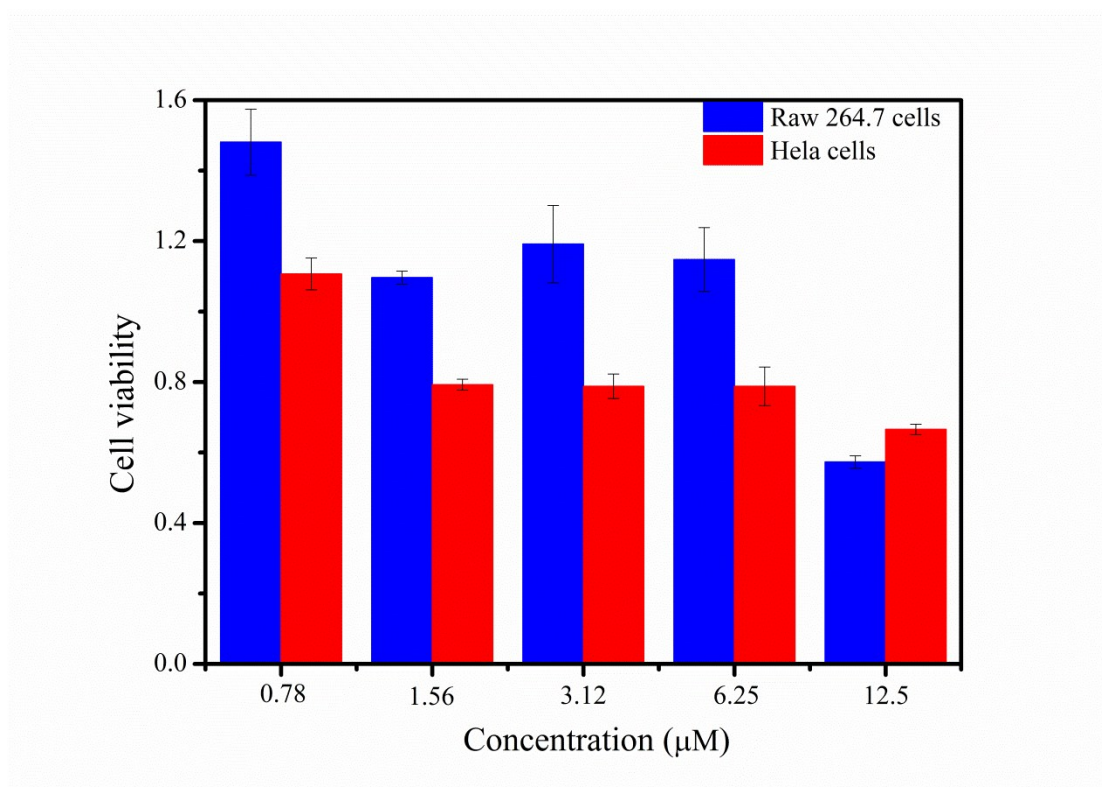


Fig. S7 Cytotoxicity data of PDAM-Lyso for Raw264.7 cells (blue) and HeLa cells (red).

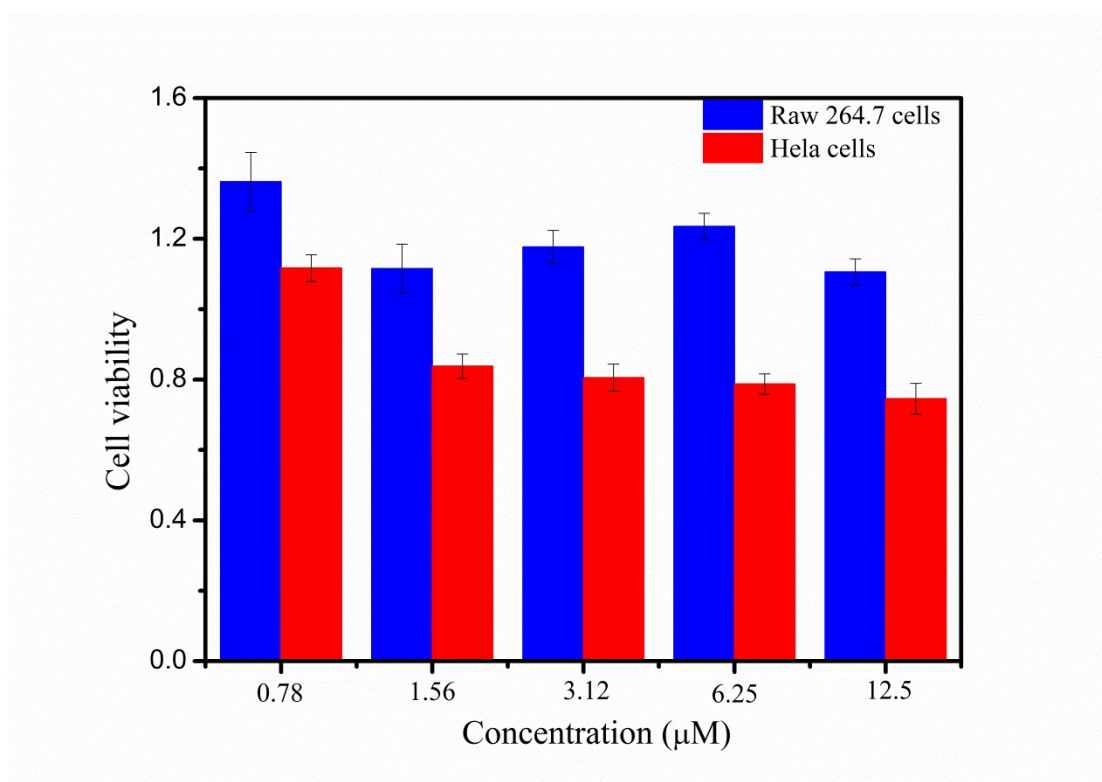


Fig. S8 Cytotoxicity data of PDAM-Me for Raw264.7 cells (blue) and HeLa cells (red).

7. Cell imaging

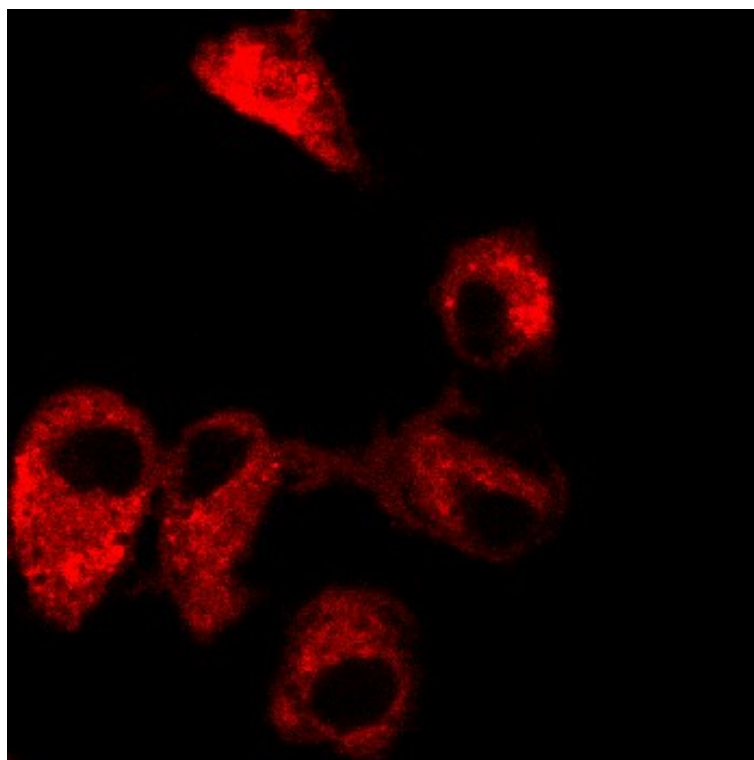


Fig. S9 Confocal fluorescent images of HeLa cells of PDAM-Lyso and Lyso-Tracker red ($\lambda_{\text{ex}} = 405$ nm, $\lambda_{\text{em}} = 560 - 690$ nm).

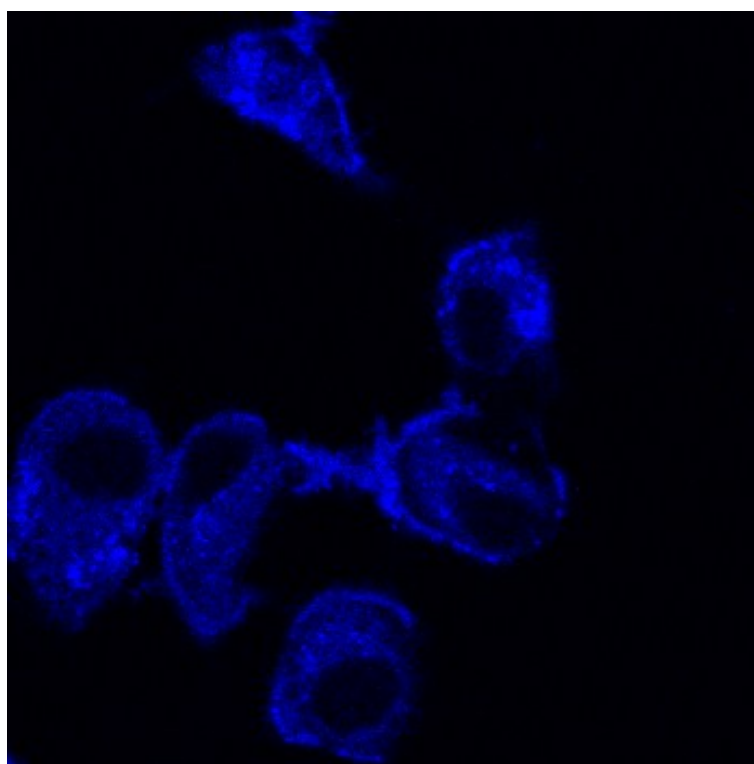


Fig. S10 Confocal fluorescent images of HeLa cells of PDAM-Lyso and Lyso-Tracker red ($\lambda_{\text{ex}} = 405$ nm, $\lambda_{\text{em}} = 430 - 560$ nm).

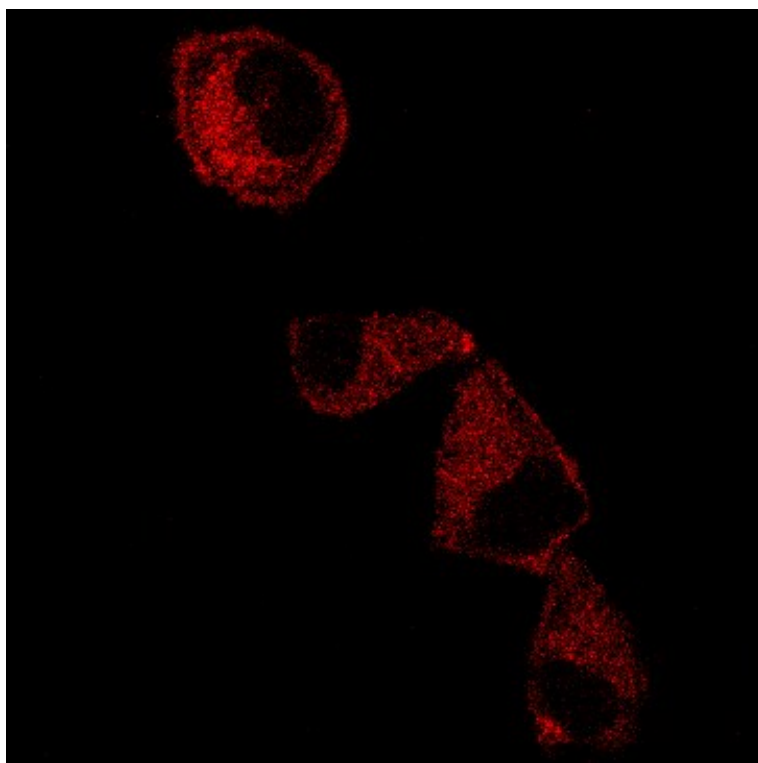


Fig. S11 Confocal fluorescent images of HeLa cells of PDAM-Me and Lyso-Tracker red ($\lambda_{\text{ex}} = 405$ nm, $\lambda_{\text{em}} = 560 - 690$ nm).

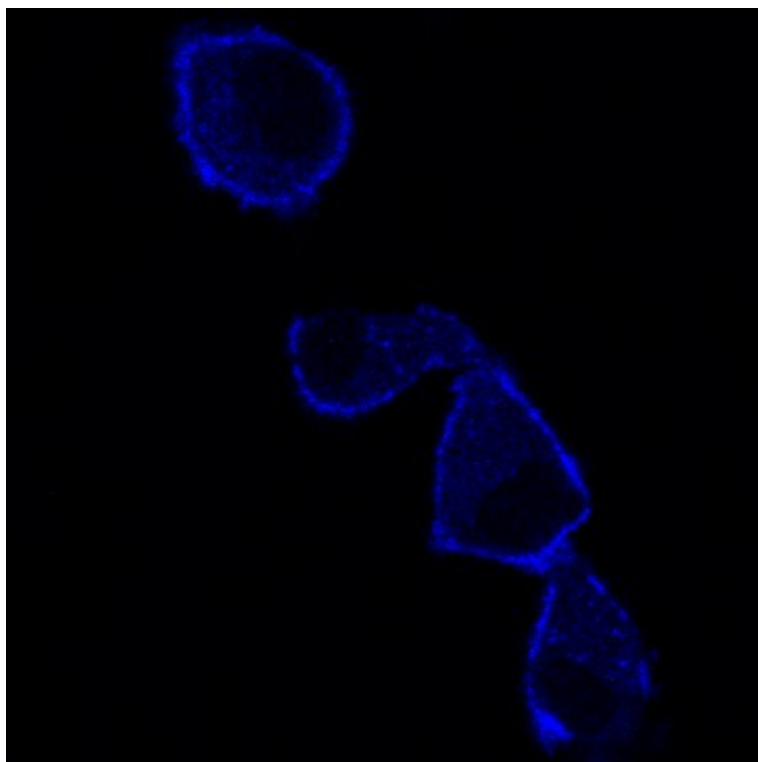


Fig. S12 Confocal fluorescent images of HeLa cells of PDAM-Me and Lyso-Tracker red ($\lambda_{\text{ex}} = 405$ nm, $\lambda_{\text{em}} = 430 - 560$ nm).

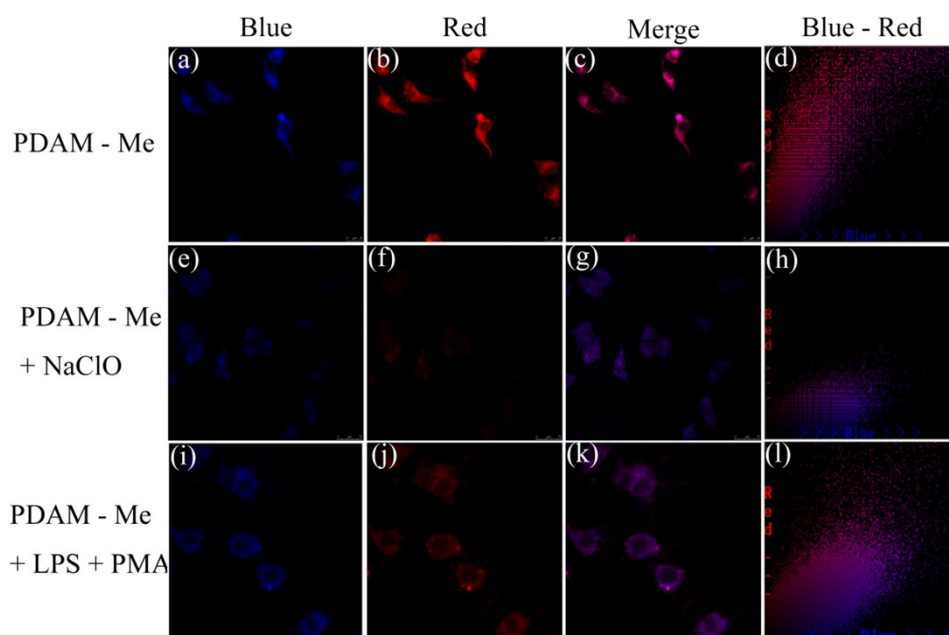


Fig. S13 Confocal fluorescence images of PDAM-Me in cells ($\lambda_{\text{ex}} = 410 \text{ nm}$). (a) HeLa cells, PDAM-Me ($3.0 \mu\text{M}$), $420 - 550 \text{ nm}$; (b) HeLa cells, PDAM-Me ($3.0 \mu\text{M}$), $570 - 700 \text{ nm}$; (c) The overlay of (a) and (b); (d) The scatter distributing plot of (c). (e) HeLa cells, PDAM-Me ($3.0 \mu\text{M}$), NaClO ($60 \mu\text{M}$), $420 - 550 \text{ nm}$; (f) HeLa cells, PDAM-Me ($3.0 \mu\text{M}$), NaClO ($60 \mu\text{M}$), $570 - 700 \text{ nm}$; (g) The overlay of (e) and (f); (h) The scatter distributing plot of (g). (i) Raw 264.7 cells, PDAM-Me ($3.0 \mu\text{M}$), LPS ($1.0 \mu\text{g/mL}$), PMA ($1.0 \mu\text{g/mL}$), $420 - 550 \text{ nm}$; (j) Raw 264.7 cells, PDAM-Me ($3.0 \mu\text{M}$), LPS ($1.0 \mu\text{g/mL}$), PMA ($1.0 \mu\text{g/mL}$), $570 - 700 \text{ nm}$; (k) The overlay of (i) and (j); (l) The scatter distributing plot of (k).

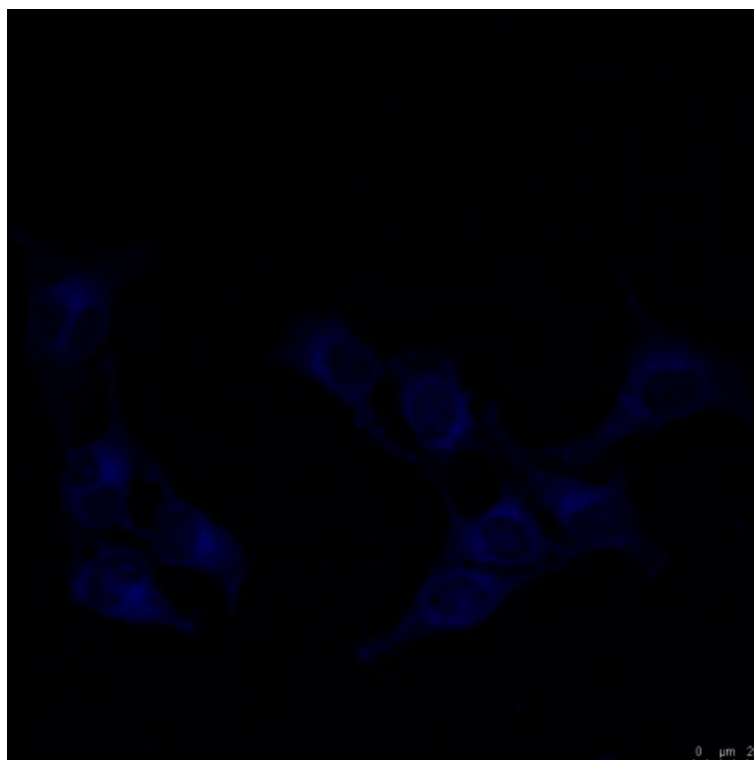


Fig. S14 Confocal fluorescent images of PDAM-Lyso (3.0 μM) in HeLa cells ($\lambda_{\text{ex}} = 410 \text{ nm}$, $\lambda_{\text{em}} = 420 - 550 \text{ nm}$).

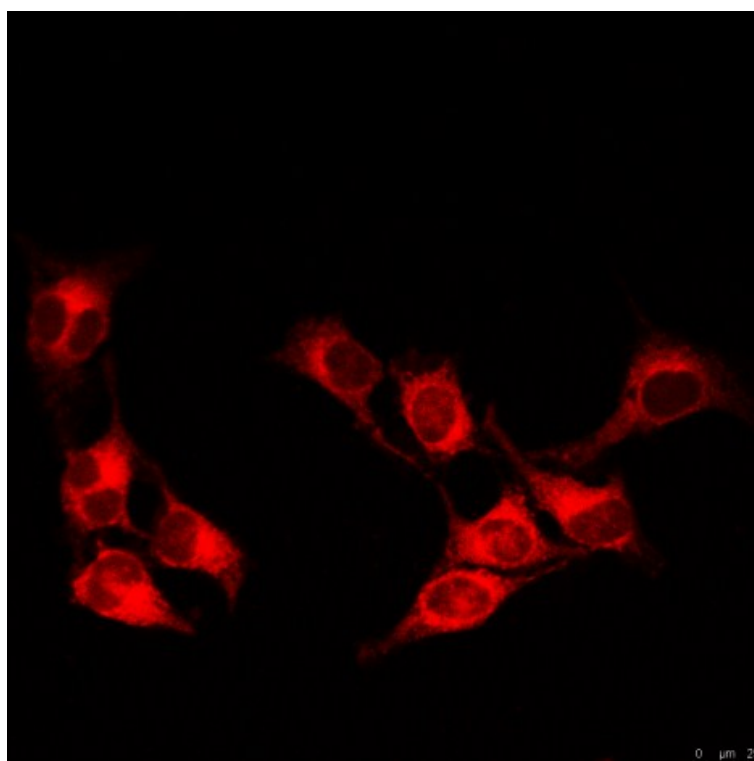


Fig. S15 Confocal fluorescent images of PDAM-Lyso (3.0 μM) in HeLa cells ($\lambda_{\text{ex}} = 410 \text{ nm}$, $\lambda_{\text{em}} = 570 - 700 \text{ nm}$).

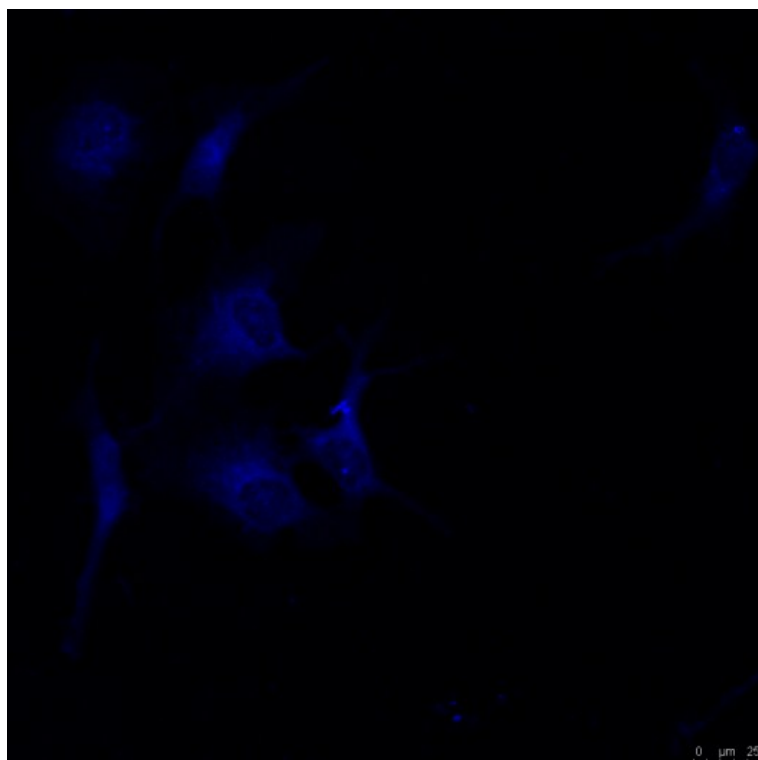


Fig. S16 Confocal fluorescent images of PDAM-Lyso (3.0 μM) in HeLa cells with the existence of NaClO (60 μM) ($\lambda_{\text{ex}} = 410 \text{ nm}$, $\lambda_{\text{em}} = 420 - 550 \text{ nm}$).

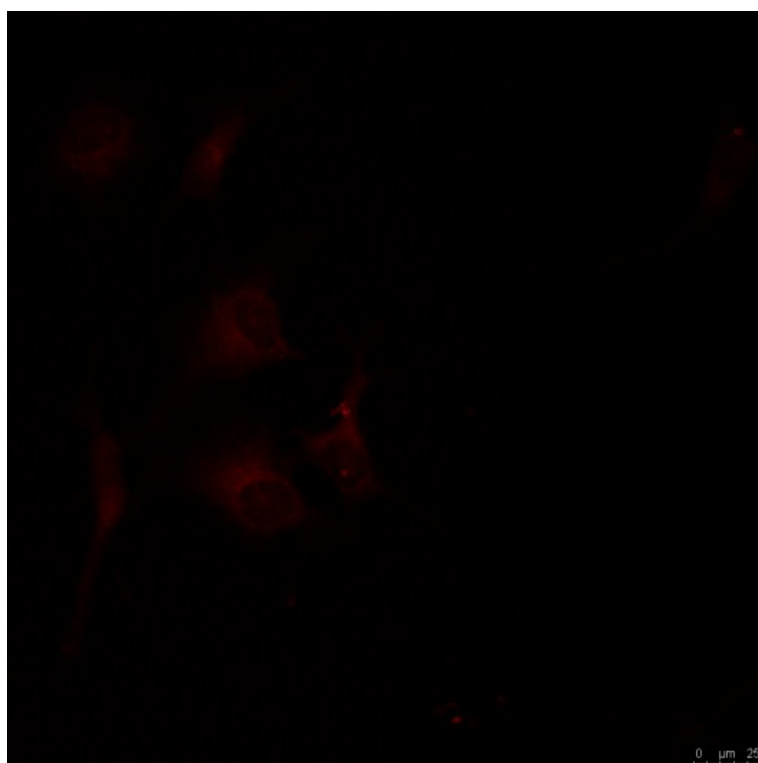


Fig. S17 Confocal fluorescent images of PDAM-Lyso (3.0 μM) in HeLa cells with the existence of NaClO (60 μM) ($\lambda_{\text{ex}} = 410 \text{ nm}$, $\lambda_{\text{em}} = 570 - 700 \text{ nm}$).

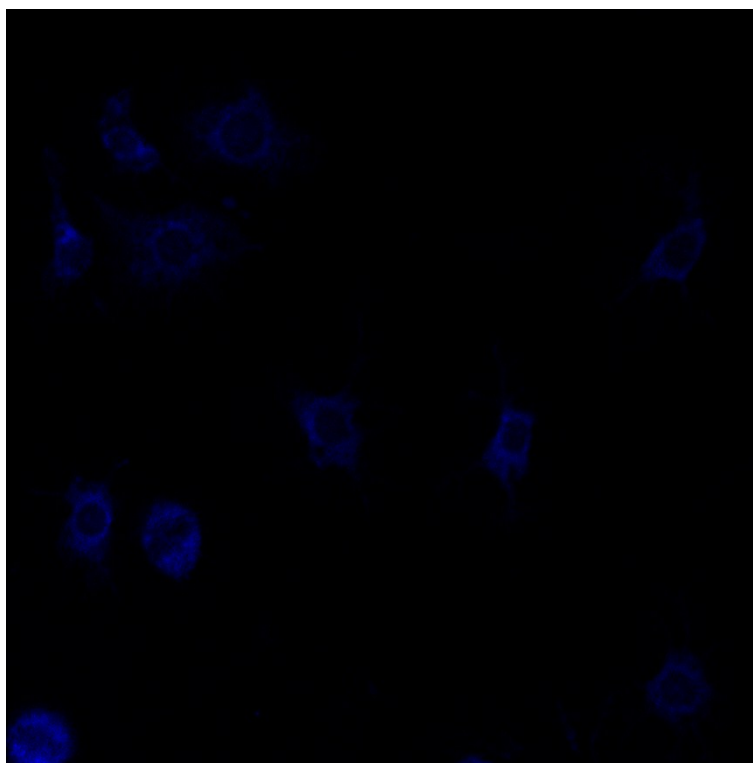


Fig. S18 Confocal fluorescent images of PDAM-Lyso (3.0 μM) in Raw 264.7 cells with LPS (1.0 $\mu\text{g/mL}$) and PMA (1.0 $\mu\text{g/mL}$) cells ($\lambda_{\text{ex}} = 410 \text{ nm}$, $\lambda_{\text{em}} = 420 - 550 \text{ nm}$).

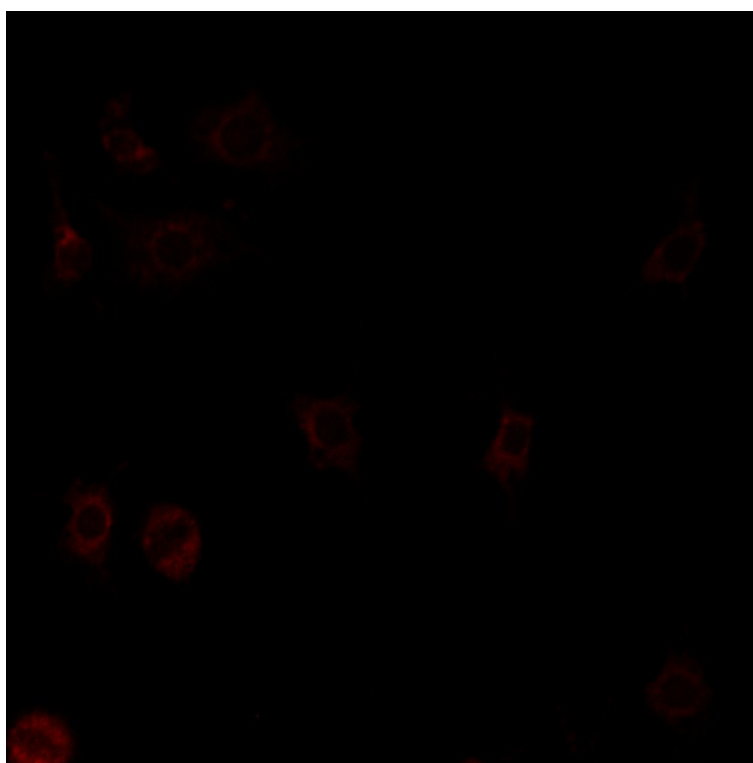


Fig. S19 Confocal fluorescent images of PDAM-Lyso (3.0 μM) in Raw 264.7 cells with LPS (1.0 $\mu\text{g/mL}$) and PMA (1.0 $\mu\text{g/mL}$) cells ($\lambda_{\text{ex}} = 410 \text{ nm}$, $\lambda_{\text{em}} = 570 - 700 \text{ nm}$).

8. Crystal data of PDAM-Me

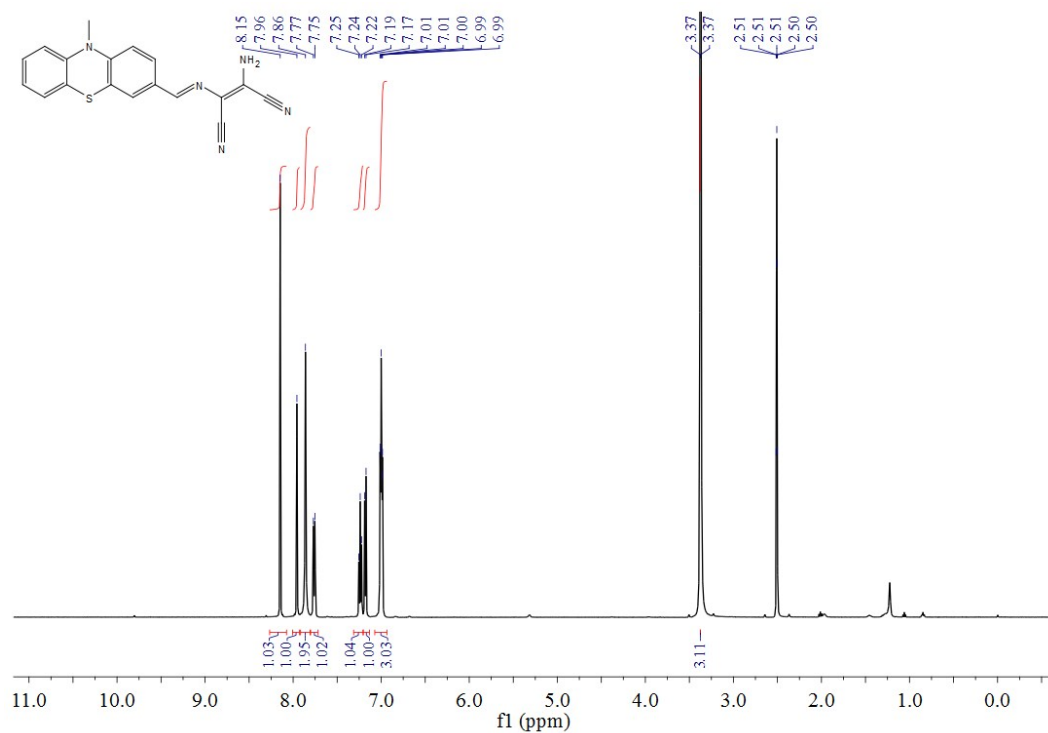
Table S1 Crystal data of compound PDAM-Me

Compound	PDAM-Me
Empirical formula	C ₁₈ H ₁₃ N ₅ S
Formula weight	331.39
Crystal system	monoclinic
Space group	<i>P</i> 2 ₁ / <i>c</i>
<i>a</i> [Å]	18.09(2)
<i>b</i> [Å]	6.977(9)
<i>c</i> [Å]	13.863(19)
α [°]	90
β [°]	109.407(12)
γ [°]	90
<i>V</i> [Å ³]	1650(4)
<i>Z</i>	4
<i>T</i> [K]	291(2)
<i>D</i> _{calcd} [g·cm ⁻³]	1.334
<i>F</i> (000)	688
μ [mm ⁻¹]	0.205
θ range[°]	2.388 - 24.999
<i>R</i> ₁	0.1562
<i>wR</i> ₂	0.4408
<i>S</i>	1.124

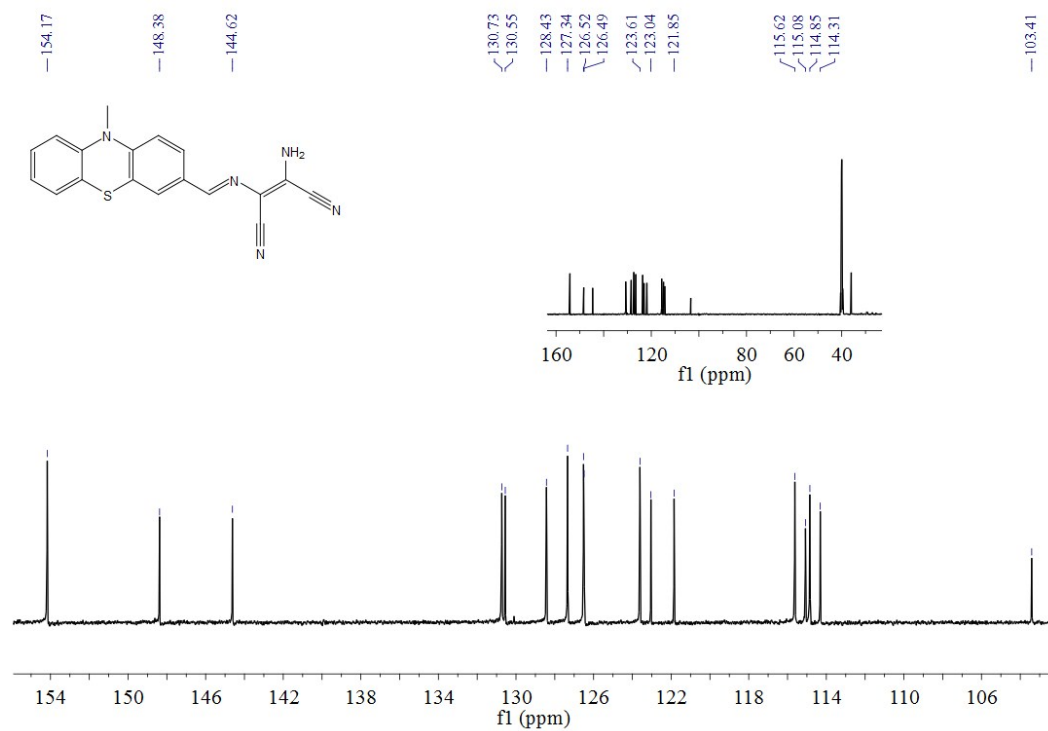
Table S2 Intermolecular hydrogen bonding parameters (Å, °) in PDAM-Me

D–H···A	D–H	H···A	D···A (<i>d</i>)	\angle DHA	Symmetry code
N5–H5A···N3	0.86	2.22	3.031(15)	157	<i>x</i> , -1+ <i>y</i> , <i>z</i>
N5–H5B···N4	0.86	2.19	3.028(14)	166	- <i>x</i> , -1/2+ <i>y</i> , 1/2- <i>z</i>

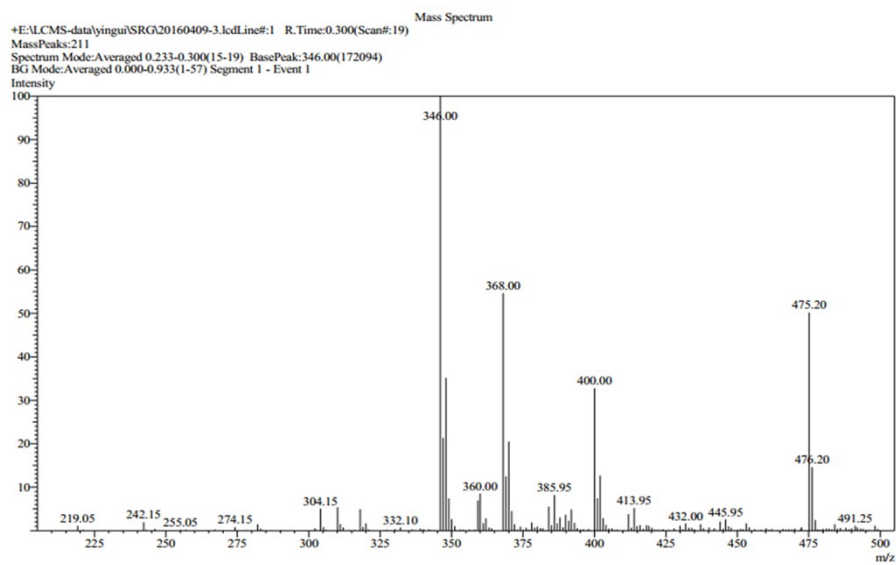
9. Supplemental spectra



¹H NMR spectrum of PDAM-Me.

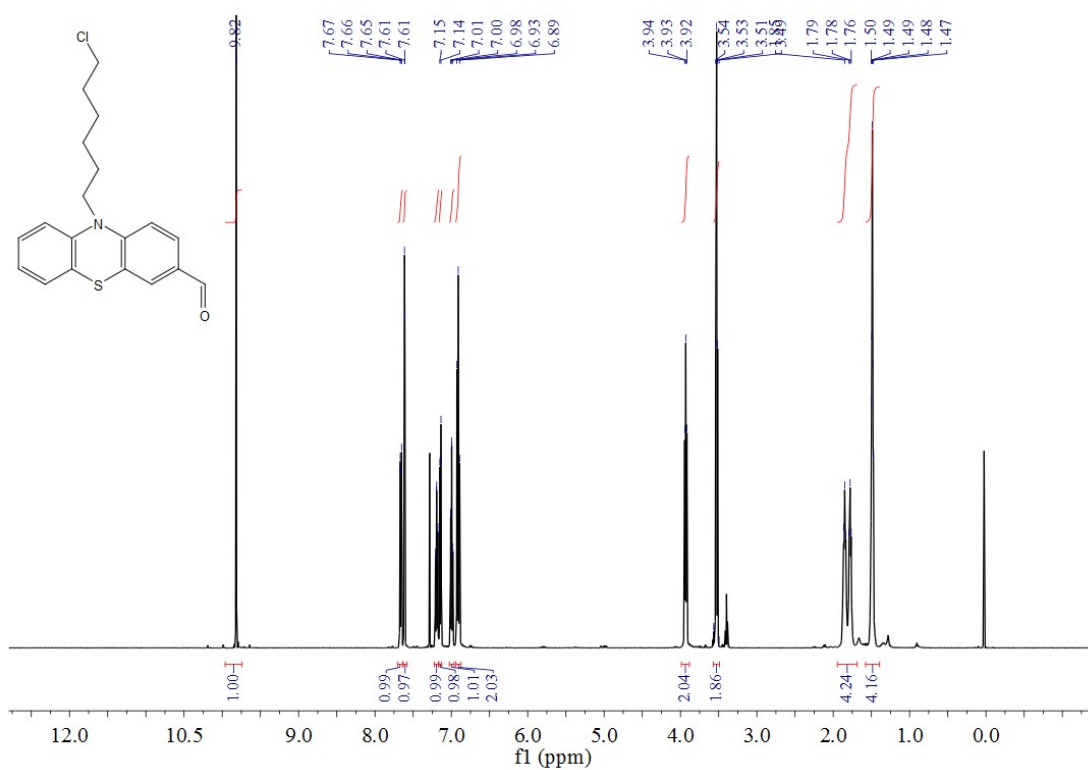


¹³C NMR spectrum of PDAM-Me.

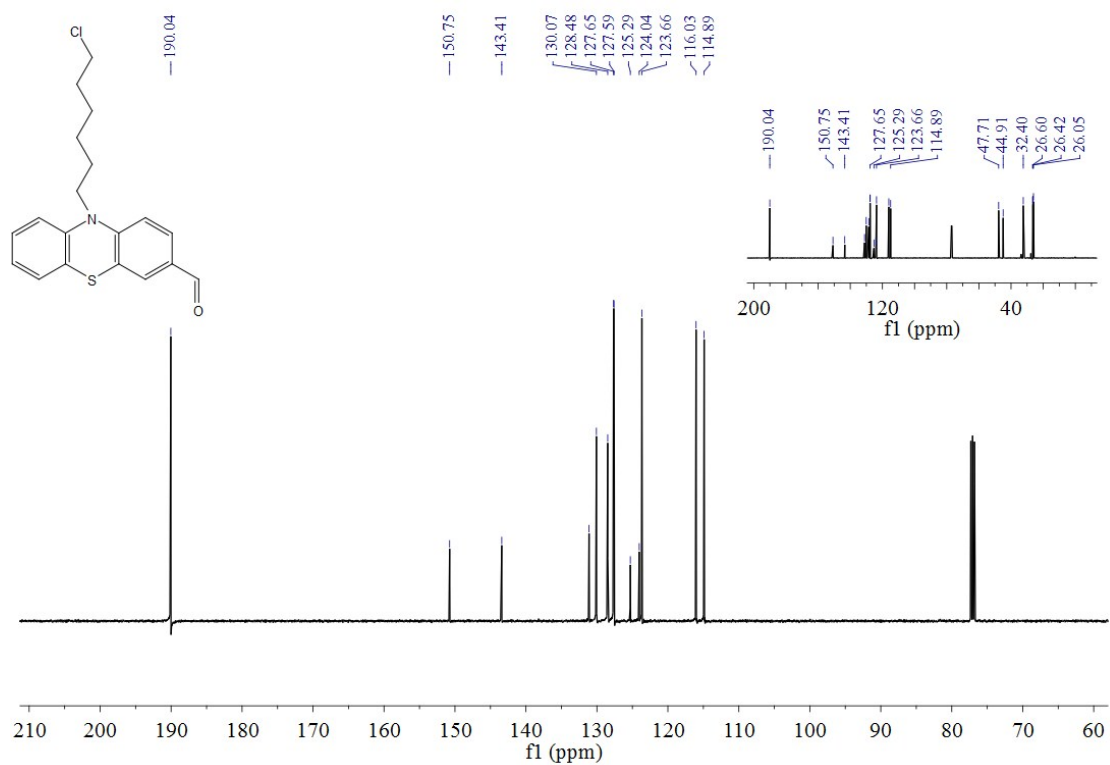


ESI

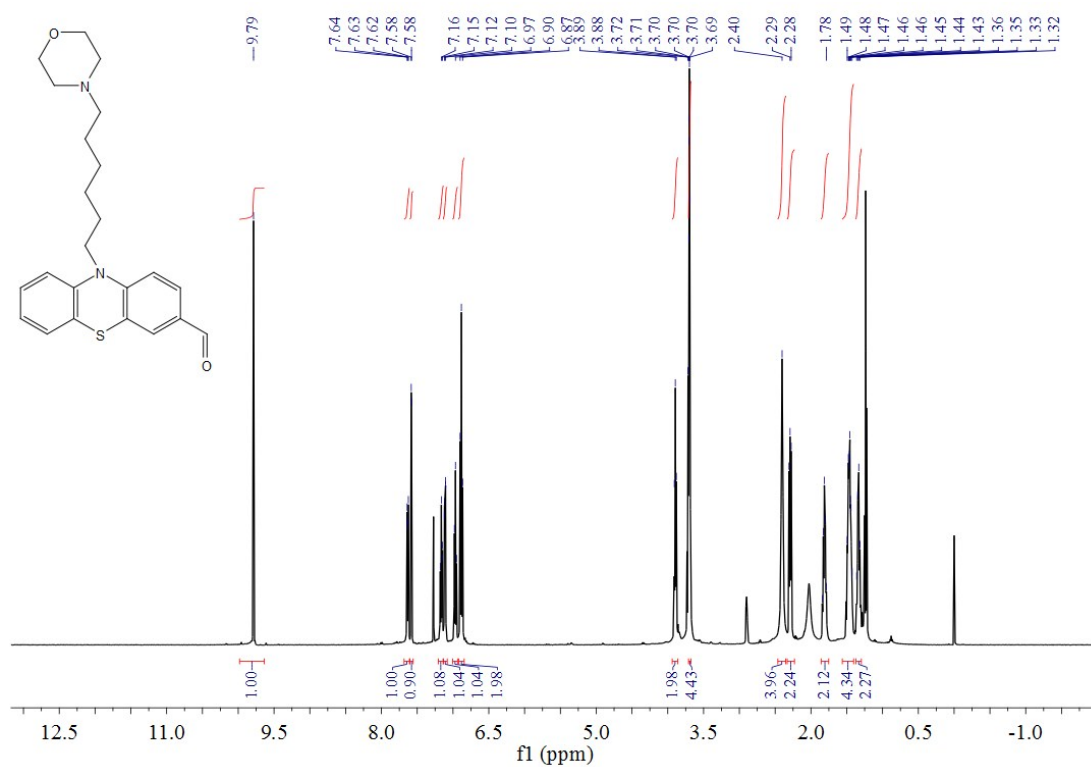
-MS spectrum of the compound 4.



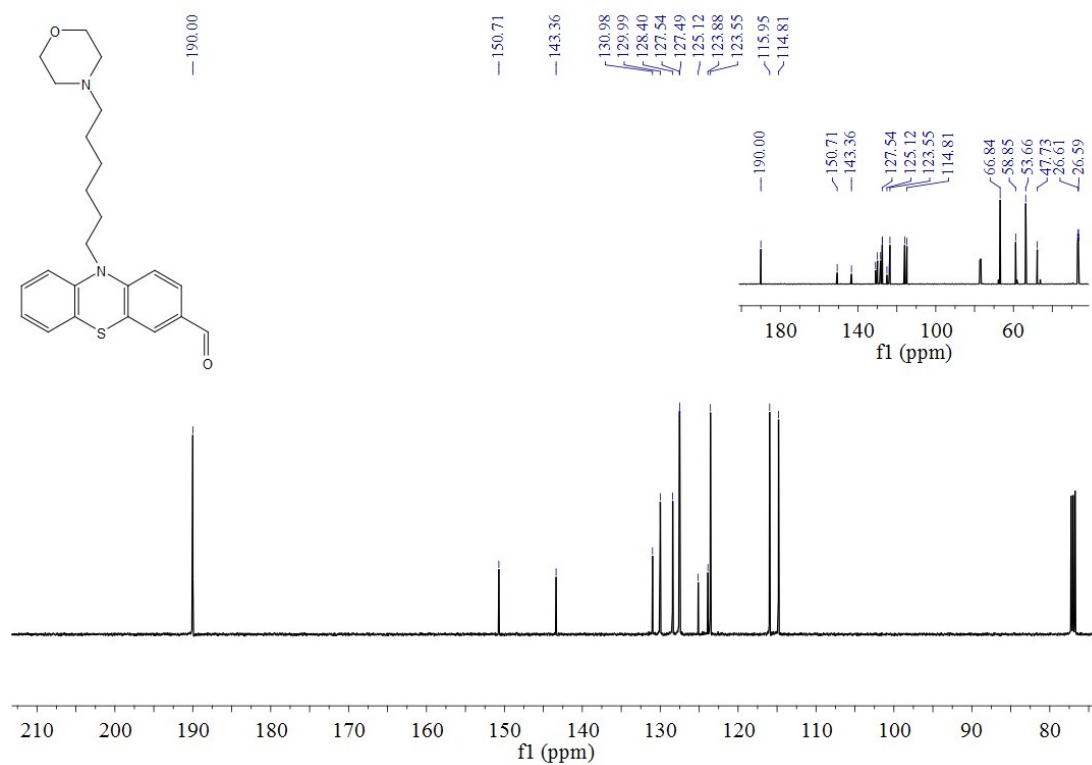
¹H NMR spectrum of compound 4.



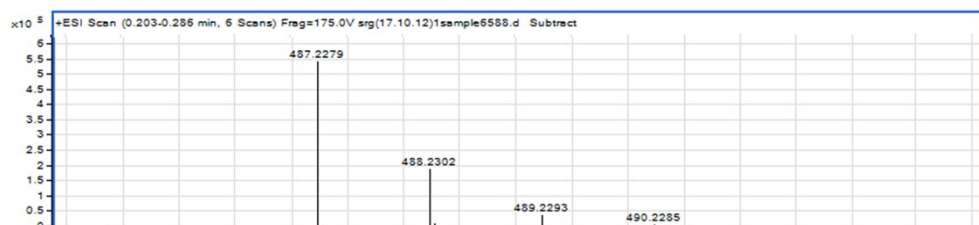
^{13}C NMR spectrum of compound 4.



^1H NMR spectrum of compound 5.

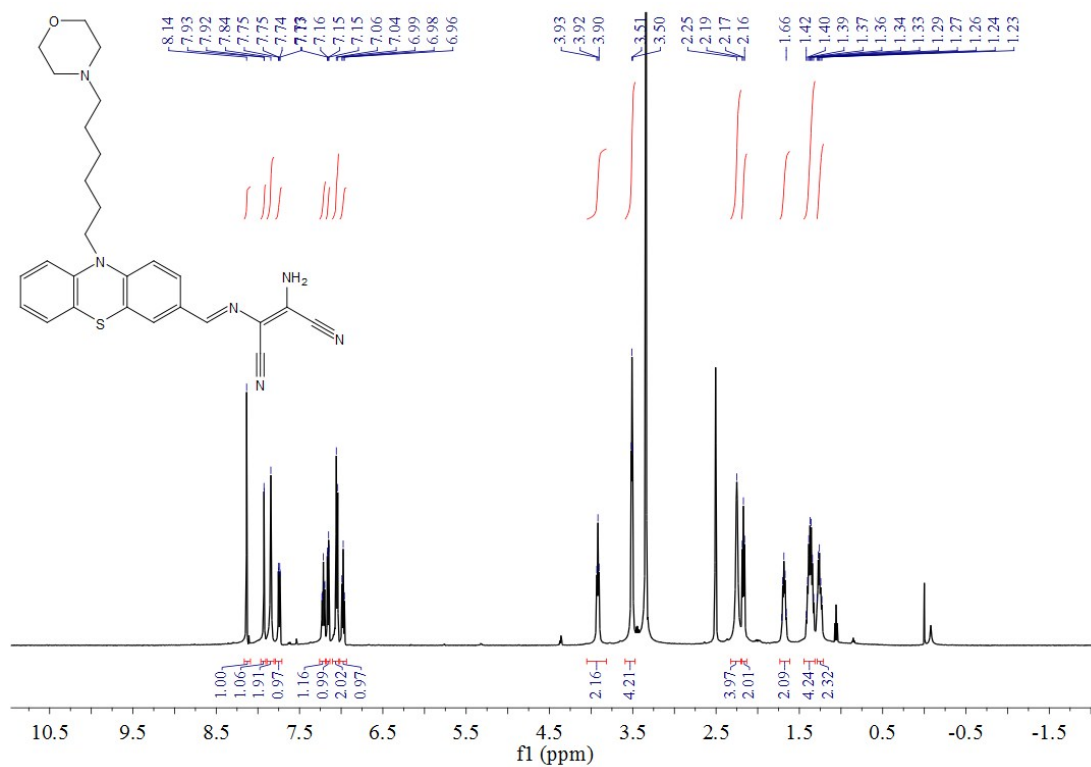


¹³C NMR spectrum of compound 5.

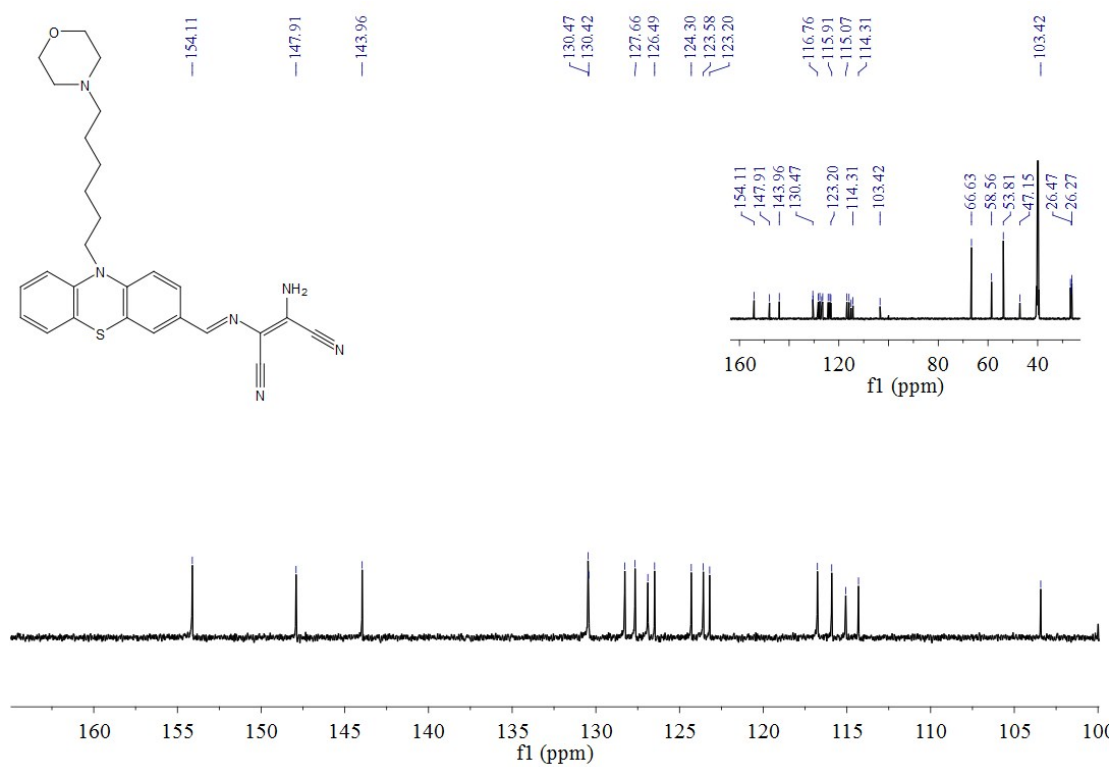


-MS spectrum (positive) of PDMA-Lyso.

HR



¹H NMR spectrum of PDMA-Lyso.



¹³C NMR spectrum of PDMA-Lyso.